Deactivation of Rhodopsin in the Transition from the Signaling State Meta II to Meta III Involves a Thermal Isomerization of the Retinal Chromophore C═N Double Bond†

Reiner Vogel,*,‡ Friedrich Siebert,‡ Gerald Mathias,§ Paul Tavan,§ Guibao Fan,|| and Mordechai Sheves||

Biophysics Group, Institut für Molekulare Medizin und Zellforschung, Albert-Ludwigs-Universität Freiburg, Hermann-Herder-Strasse 9, D-79104 Freiburg, Germany, BioMolekulare Optik, Sektion Physik, LMU München, Oettingenstrasse 67, D-80538 München, Germany, and Department of Organic Chemistry, Weizmann Institute of Science, Rehovot 76100, Israel

Received April 29, 2003; Revised Manuscript Received June 11, 2003

ABSTRACT: Light-induced isomerization of rhodopsin's retinal chromophore to the activating all-trans geometry initializes the formation of the active receptor state, Meta II. In the absence of peripheral regulatory proteins, the activity of Meta II is switched off spontaneously by two independent pathways: either by hydrolysis of the retinal Schiff base and dissociation of the light receptor into apoprotein opsin plus free retinal or by formation of Meta III, an inactive species with intact retinal protonated Schiff base absorbing at 470 nm. By FTIR spectroscopy on rhodopsin reconstituted with isotopically labeled chromophores in combination with quantum mechanical DFT calculations, we show that the deactivating step during formation of Meta III involves a thermal isomerization of the chromophore C═N double bond, such that the chromophore in Meta III is all-trans-15-syn. This isomerization step is catalyzed by the protein environment and proceeds via Meta I, as suggested by its dependence on pH and on properties of the lipid/detergent environment of the protein. In the long term, Meta III decays likewise to opsin and free retinal by slow hydrolysis of the Schiff base.

Rhodopsin is the light receptor responsible for dim light vision in rod photoreceptor cells and is considered the best studied visual pigment. It is a member of the family A of the large group of G protein-coupled receptors (GPCRs)[1] and serves as a prototype to elucidate the molecular details responsible for their activation (*1*−*4*). Rhodopsin is an integral membrane protein with seven membrane-spanning α-helices, which form the apoprotein opsin. In contrast to other GPCRs, rhodopsin as a light receptor has bound its light-sensing chromophore, 11-*cis*-retinal, covalently via a protonated Schiff base to a lysine residue, Lys-296, in the transmembrane section of helix 7. Upon photon absorption, this chromophore isomerizes within 200 fs to an all-trans geometry (*5*). This initial isomerization step triggers a slower protein response which subsequently leads to formation of the activated receptor state, Meta II, that is capable of interacting with its cognate G protein, transducin, and other downstream elements of the signal transduction cascade.

Once activated, the receptor has to be shut off again. In the photoreceptor cell, this is accomplished by rapid binding of rhodopsin kinase, which caps the receptor and phosphorylates mainly cytoplasmic serines, and eventual binding of arrestin to the phosphorylated receptor, thereby preventing its interaction with transducin and further activation of the signal transduction cascade. This deactivation of the single receptor molecule takes place on the time scale of 100 ms to seconds (*6*, *7*) and confers the eye a reasonable time resolution. However, there are as well other mechanisms that lead to deactivation of Meta II and that do not depend on the presence of these regulatory proteins. In the outer segments of rod photoreceptor cells, rhodopsin is contained in stacks of disk membranes. These disk membranes can be isolated and hypotonically washed such that their protein content consists almost exclusively of rhodopsin embedded in its native membrane environment (*8*). In isolated disk membranes, the activity of Meta II is shut off by two independent processes intrinsic to rhodopsin itself. The first one involves hydrolysis of the retinal Schiff base linkage and dissociation of the receptor molecule into the apoprotein opsin and free all-*trans*-retinal. This process occurs on the time scale of minutes at room temperature. In the absence of all-*trans*-retinal in the retinal binding pocket, opsin adopts a conformation which is largely inactive toward transducin (for a summary see ref *9*) and close to that of the initial dark state (*10*, *11*). Only at very low pH values is opsin capable of adopting an active state conformation similar to that of Meta II (*12*). This process is characterized by a pK_a

† This work was supported by grants from the DFG (Si 278/16-3,4 to F.S., SFB 533/C3 to P.T.), Fonds der Chemischen Industrie (to F.S.), Volkswagen Stiftung (project I/73 224 to P.T.), the A.M.N. Fund for the Promotion of Science, Culture and Arts in Israel (to M.S.), and the Israel National Science Foundation (Grant 659/00 to M.S.). M.S. holds the Katzir-Makineni professorial chair in chemistry.

* Corresponding author: phone, +49 761 203 5391; fax, +49 761 203 5390; e-mail, reiner.vogel@biophysik.uni-freiburg.de.

‡ Albert-Ludwigs-Universität Freiburg.

§ LMU München.

|| Weizmann Institute of Science.

[1] Abbreviations: GPCR, G protein-coupled receptor; FTIR, Fourier transform infrared; DFT, density functional theory; pRSB, protonated retinal Schiff base; DM, dodecyl maltoside.

10.1021/bi034684+ CCC: $25.00
Published on Web 08/02/2003

around 4. The alternative process involves the formation of Meta III, which absorbs around 470 nm (*13*−*16*). Meta III formation can be observed under more alkaline conditions in parallel to hydrolysis and makes up about 30% of the decay product at pH 8.0. Meta III itself decays slowly by hydrolysis into free retinal and opsin on longer time scales.

What is the true nature of Meta III? Meta III is intrinsically difficult to study as there are no conditions where exclusively Meta III is formed during the decay of the Meta I/Meta II photoproduct equilibrium. Instead, dissociation of the receptor into opsin and free retinal was under all tested conditions the predominant decay pathway. Besides Meta III, there will therefore always be free all-*trans*-retinal absorbing at 380 nm in the decay mixture, as well as Schiff bases of all-*trans*-retinal, which are spontaneously formed with peripheral amino groups of opsin or of lipids, namely, of ethanolamine (*17*). These peripheral Schiff bases of retinal are expected to absorb at either 365 or 440 nm, depending on whether their Schiff base nitrogen is deprotonated or protonated. Previous studies on Meta III have verified that the retinal chromophore is still in its binding pocket by using circular dichroism (*16*) and by investigating Meta III's photochemistry (*18*). A recent study by Heck et al. further characterized formation of Meta III (*19*). They confirmed that Meta III has an inactive protein conformation and that it can be photoconverted to a 380 nm species which is likely to be identical to Meta II (*20*). This allows to distinguish Meta III from peripheral Schiff bases of released retinal and offers the opportunity to study Meta III in more detail.

One important question could, up to now, not be answered by any of these studies: What triggers the transition from Meta II to Meta III and initiates thereby the structural changes that can be observed during this transition and that lead to the deactivation of the protein?

We have used in this study FTIR spectroscopy on rhodopsin reconstituted with isotopically labeled retinals to examine in detail the structure of the chromophore in Meta III. The FTIR experiments were combined with quantum chemical calculations and retinal extraction experiments. The results indicate that formation of Meta III is triggered by a thermal isomerization of the chromophore. The Schiff base C═N double bond, which is in an anti conformation in Meta I and Meta II, is found in a syn geometry in Meta III. The fate of the retinal chromophore during decay of the Meta I/Meta II pool is therefore twofold: it can leave its binding pocket and thereby allow the apoprotein to adopt an energetically more favorable inactive conformation. Alternatively, it can comply to the protein environment and adopt a different isomer which is compatible with the binding pocket in such an inactive protein conformation.

MATERIALS AND METHODS

Pigment Preparation. Rhodopsin in washed disk membranes was prepared from cattle retinae according to standard procedures (*8*) and stored at −80 °C. Preparation of rhodopsin with isotopically labeled chromophores was accomplished by regenerating opsin with synthetic retinals as described previously (*21*), followed by extraction of excess retinal by cyclodextrin (*22*, *23*). Isotopically labeled retinals were a generous gift of J. Lugtenburg. Permethylated disk membranes were prepared by two rounds of methylation with formaldehyde and pyridine borane as described previously (*24*). Successful permethylation was checked by adding retinal to the treated disk membranes at acidic pH and indicated by lack of additional absorption at 440 nm due to formation of peripheral protonated Schiff bases. Pigment in detergent was prepared either by concanavalin A affinity chromatography (*25*) in the case of dodecyl maltoside or by solubilizing washed disk membranes in excess detergent in the case of digitonin.

FTIR Spectroscopy. FTIR spectroscopy was performed with a Bruker IFS 28 spectrometer with an MCT (mercury cadmium telluride) detector. IR spectra were recorded in blocks of 512 scans with a spectral resolution of 4 cm^{-1} and an acquisition time of 1 min and corrected for temporal baseline drifts. Experiments were performed with sandwich samples with 0.5 nmol of pigment that were prepared as described in detail elsewhere (*2*, *12*). As buffers, we used 200 mM citric acid, MES (2-*N*-morpholinoethanesulfonic acid), and BTP (Bis-Tris-propane), in overlapping ranges, containing 200 mM NaCl. For H/D exchange at the Schiff base, we twice equilibrated the sample film with D_2O and dried it under nitrogen before adding the respective buffer prepared in D_2O.

Samples were photolyzed for 30 s through a fiber optics fitted to a 150 W slide projector. For the photolysis of rhodopsin, we used a 495 nm long-pass filter, while for the photolysis of Meta III, a 475 nm long-pass filter was used instead. All experiments were performed at 30 °C, unless stated differently.

UV−*Visible Spectroscopy.* For UV−visible spectroscopy sandwich samples identical to the infrared samples were used in a Perkin-Elmer Lambda 17 spectrophotometer equipped with a temperature-controlled sample holder. Illumination and temperature were as in the IR experiments. Detergent samples were investigated in solutions in 100 μL microcuvettes with 10 mm path length. Membrane suspensions were examined as well in microcuvettes with a scattering blank in the reference channel of the spectrometer.

In the experiments with dodecyl maltoside and digitonin, contributions of rhodopsin and isorhodopsin arising from the photoequilibrium of the first illumination were taken into account by adding in a control experiment 10 mM hydroxylamine after the first illumination and allowing the hydroxylamine-sensitive photoproducts to bleach chemically. The amount of residual hydroxylamine-stable pigment (a mixture of mainly 9-*cis*-isorhodopsin and some 11-*cis*-rhodopsin) was determined by bleaching this control sample a second time (now in the presence of hydroxylamine). The amount of this residual pigment was found to be 17% of the total pigment in digitonin and 2% in dodecyl maltoside under our experimental conditions, with a depletion peak of this isorhodopsin/rhodopsin mixture being centered at 487 nm. These data were used to correct the spectra of the second illumination in the detergent experiments: From the spectrum of the first illumination, the position of the photoproduct equilibrium between Meta I and Meta II in each detergent was determined by fitting these spectra to three Gaussian peaks centered at 500 nm (for the rhodopsin depletion peak), 480 nm (for the Meta I photoproduct), and 380 nm (for the Meta II photoproduct) and an additional peak of fixed amplitude at 487 nm accounting for the production of the rhodopsin/isorhodopsin mixture, using Bruker's Opus soft-

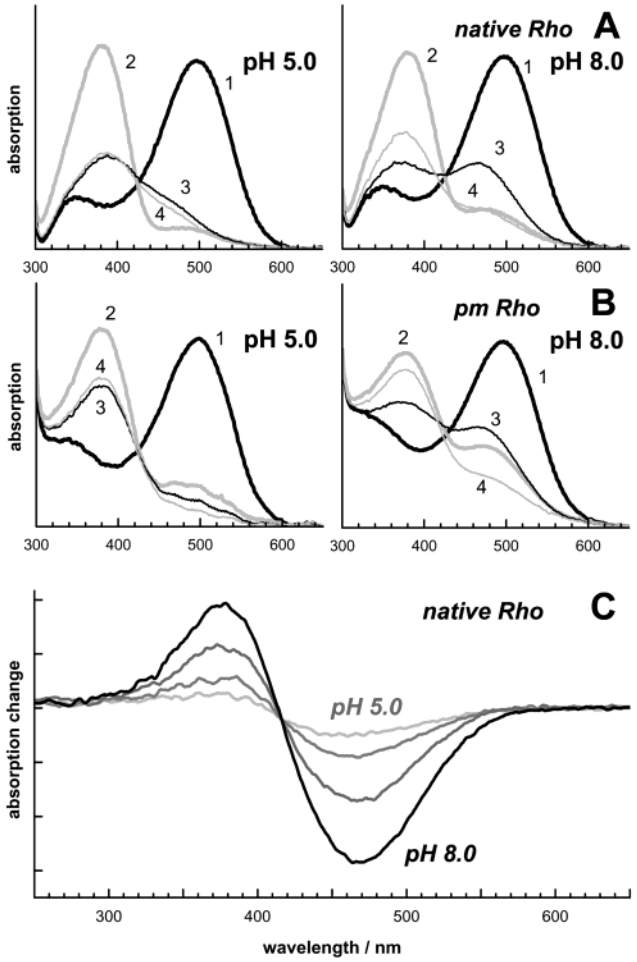

FIGURE 1: Decay of Meta II and formation of Meta III. (A) Rhodopsin in disk membranes was photolyzed at 30 °C (30 s with 495 nm long-pass) at either pH 5.0 or pH 8.0 to form largely Meta II (380 nm), which then decayed on the time scale of minutes to either free retinal (385 nm), peripheral retinal Schiff bases (440 and 370 nm), or Meta III (470 nm). Shown are the spectra of the dark state (1, 500 nm), of the photoproduct equilibrium obtained immediately after photolysis (2), and of its decay products obtained 20 min after photolysis (3). Subsequently, the nature of the decay products was probed by a second illumination (30 s with 475 nm long-pass), leading again to formation of substantial Meta II at pH 8.0 but not at pH 5.0. (B) Same as in (A) but for permethylated disk membranes. (C). Difference spectra of the second illumination (Meta III to Meta II′) for native disk membranes (spectrum 4 minus spectrum 3) for pH values 5.0, 6.0, 7.0, and 8.0 show an increasing content of the photoconvertible decay product Meta III at more alkaline pH. The difference spectra in (C) were normalized to the respective absorption of the dark state.

ware (Bruker, Ettlingen, Germany). Approximate correction spectra were calculated from these spectra by shifting the depletion peak from 500 nm (for rhodopsin) to 487 nm (for the residual rhodopsin/isorhodopsin mixture) while leaving all other parameters (peak width and amplitude) and the other peaks unchanged. The obtained spectra, multiplied by a suitable scaling factor to faithfully reflect the 17% or 2% contributions of the residual rhodopsin/isorhodopsin mixture to the photoreaction, were subtracted from the original spectra of the second illumination to eliminate contributions of this mixture and to obtain the true spectrum of the photoreaction from Meta III to the Meta I/Meta II pool only.

Quantum Chemical Calculations. For vibrational analysis of the Meta III chromophore, which is a protonated retinal Schiff base (pRSB), a model compound was used. In this model the β-ionone ring of the pRSB and the lysine side chain starting from Cδ were replaced by methyl groups (i.e., C6−C7═ ... ═N−Cϵ−Cδ). Using density functional theory (DFT) Hessian matrices and dipole gradients were calculated for four isomers, i.e., all-trans-15-syn, all-trans-15-anti, 13-cis-15-syn, and 13-cis-15-anti (for atom numbers see Figure 4 further below). Two additional counterion calculations were conducted for the two 15-syn isomers. They included a chloride ion constrained to the plane of the chromophore at a distance of 5 Å from the Schiff base nitrogen and at a Cl−N−Cϵ angle of 115°, which places the ion approximately onto the axis of the N−H bond. For DFT Becke's three parameter hybrid functional (*26*), the Lee−Yang−Parr correlation functional (*27*) (B3LYP), and the 6-31G* basis set provided by Gaussian98 (*28*) were applied. From the Hessians and the dipole gradients the normal modes, frequencies, and IR intensities of the isotopomers native, (^{13}C14,^{13}C15), ND, and (ND,^{13}C14,^{13}C15) were determined. Frequencies were scaled by the empirical factor of 0.9613, which corrects the slight overestimate of force constants by the B3LYP functional in the given basis set (*29*).

Chromophore Extraction. Hydrated films of rhodopsin (pH 7.0) were irradiated for 2 s with a 530 nm long-pass filter. The sample was immediately extracted with 500 μL of ice-cooled water followed by addition of 500 μL of hydroxylamine solution (1.0 M). The sample was vortexed for 2 min followed by addition of 1000 μL of cold ethanol (0 °C) and 2000 μL of cold hexane. The sample was vortexed for another 60 s after each addition. The mixture was then centrifuged at 14000*g* for 3 min, and the upper layer was dried by argon stream. The residue was dissolved with 20 μL of hexane and analyzed by HPLC (Purospher column, Si 5 μm, Merck). For analyzing the chromophore configuration at the Meta III stage, hydrated films of rhodopsin (pH 7.5) were irradiated for 2 s with a 530 nm long-pass filter followed by thermal decay to Meta III for 30 min. The chromophore was extracted using the same procedure.

To analyze the possibility of a thermal isomerization of the C13═C14 double bond *outside* the binding pocket, rhodopsin (pH 7.0) was incubated in the dark for 1 h at 25 °C with 1 equiv of a retinal mixture consisting of equal amounts of 13-cis and all-trans isomers. Hydrated films were prepared, extracted, and analyzed by HPLC as described above.

RESULTS

Formation of Meta III during the Decay of Meta II. Photolysis of rhodopsin in disk membranes (λ_{max} 500 nm) leads to 11-cis to all-trans isomerization of its retinal chromophore and establishes at ambient temperature within milliseconds an equilibrium between the active receptor species, Meta II (380 nm), and its still inactive precursor, Meta I (480 nm). In this equilibrium, Meta II is favored by higher temperature and lower pH (*30*). We performed our experiments at 30 °C, such that Meta II is the predominant photoproduct over the assayed pH range, with contributions of Meta I becoming notable only at pH 8.0. This is shown in Figure 1A. Meta II decays subsequently with a half-time of about 2.8 min between pH 5.0 and pH 7.0 (*12*) and with a slightly faster half-time of 2.0 min at pH 8 such that the

spectra become stationary within 20 min after photolysis of the sample (spectrum 3 in Figure 1A). In principle, the decay product may consist of up to four spectroscopically different species: Meta III, absorbing at 470 nm, free all-*trans*-retinal (380 nm), and protonated and deprotonated peripheral Schiff bases of released retinal. Under the term "peripheral Schiff bases", we combine Schiff bases of released retinal with any of the 10 cytoplasmic or extracellular lysine residues of opsin different from Lys-296 or with the amino groups of the ethanolamine content of the membrane moiety (*17*). These peripheral Schiff bases absorb at 440 or at 365 nm, depending on whether they are protonated or not. To distinguish between these four species, we prepared permethylated disk membranes (*24*) in which all available amino groups are methylated except for the active site Lys-296, which forms the Schiff base with retinal in the binding pocket. Formation of peripheral Schiff bases with free retinal is thereby prevented such that we expect to observe only free retinal and Meta III as decay products of Meta II. This is indeed the case as shown in Figure 1B. At pH 5.0, the decay product (spectrum 3) consists almost exclusively of free retinal, while at pH 8.0, there are considerable contributions of Meta III, as evident from the pronounced 470 nm peak. However, compared to the native system, permethylation perturbs the biochemical properties of the disk membranes. This perturbation leads to an increased yield of Meta I at the expense of Meta II, which becomes particularly evident at pH 8.0 (spectra 2 in Figure 1A,B).

Upon photolysis of the decay products with a 475 nm longpass filter, we can efficiently convert Meta III back to Meta II (*19*, *20*), while free retinal and peripheral Schiff bases show only little photochemistry (spectra 4 in Figure 1A,B). This allows us to continue studying Meta III with native disk membranes and to use permethylated membranes only for additional control experiments. By calculating the difference spectra between spectra 3 and 4, we can quantify the yield of Meta III during the decay process as a function of pH (Figure 1C), which is highest at alkaline pH. For clarity only, we will in the following distinguish between Meta II formed directly from the dark state and Meta II obtained by photolysis of Meta III and will term the latter Meta II′. Biochemically, both species are likely identical and show, for instance, a similar p*K* of their equilibria with their respective Meta I species, as will be shown further below.

FTIR Spectroscopy of Meta III. To obtain more information on the properties of both the protein and the chromophore moiety in Meta III, we repeated these experiments with FTIR difference spectroscopy and recorded dark state to Meta II and subsequently Meta III to Meta II′ difference spectra, which are shown in panels A and B of Figure 2. In the Meta III to Meta II′ spectra, the difference bands in the amide I and II range around 1650 and 1550 cm^{-1}, respectively, as well as the characteristic pattern of C═O stretch vibrations of protonated carboxylic acids above 1700 cm^{-1} which very much resemble those observed in the dark state to Meta II difference spectra (*2*, *31*). In particular, the positive band at 1713 cm^{-1} in the dark state to Meta II difference spectra reflects the protonation of Glu-113, which serves as the counterion to the protonated Schiff base in the dark state, during the transition to Meta II (*32*, *33*). The identical band in the Meta III to Meta II′ difference spectra therefore indicates that Glu-113 should be charged in Meta III. In summary, the protein conformation of Meta III can be expected to be inactive. It is similar to but not identical with that of the dark state, as the latter is stable in the presence of hydroxylamine, while Meta III is not (see below).

Similarly, as already shown by UV−visible difference spectra in Figure 1C, the amplitude of the Meta III to Meta II′ spectra increases with increasing pH, reflecting a pH dependence of the Meta III yield during Meta II decay. By using the −1768/+1748 cm^{-1} difference band of Asp-83 (*34*, *35*) as a marker, the amount of Meta III being formed at the different pH values can be determined to be 5% at pH 5.0, 11% at pH 6.0, 18% at pH 7.0, and 30% at pH 8.0.

Despite obvious similarities between Meta III and the dark state of rhodopsin regarding the conformation of the protein, the structure of the chromophore must be different, as the pattern of the fingerprint bands of retinal between 1300 and 1050 cm^{-1} is considerably altered (Figure 2B). These bands consist of combinations of mainly C−C stretching and CH bending vibrations, and their intensities and positions characterize the isomeric state of the chromophore (*31*, *36*). The three negative fingerprint bands at 1201, 1181, and 1158 cm^{-1}, as well as the negative 1349 cm^{-1} band, can be attributed to Meta III. There is little interference with corresponding (positive) fingerprint bands of the Meta II photoproduct states in Figure 2, as the intensity of C−C stretching vibrations decreases very much if the Schiff base becomes deprotonated (*37*), which is the case in Meta II. In control experiments with permethylated disk membranes, the same Meta III fingerprint pattern as with native disk membranes was produced, indicating only little interference by potential photochemistry of protonated peripheral Schiff bases (data not shown).

Analysis of the Fingerprint Bands in Meta III. Next we aimed at determining the isomeric state of the chromophore in Meta III by its fingerprint bands. We first tested the sensitivity of the fingerprint pattern on H/D exchange at the protonated Schiff base (Figure 3A) and noticed a disappearance of the 1181 cm^{-1} band and appearance of a doublet at 1247 and 1236 cm^{-1} in D_2O. In addition, the strong reduction of the negative band at 1349 cm^{-1} is remarkable. We repeated this experiment with rhodopsin reconstituted with retinals that were ^{13}C-labeled at C14 and at both C14 and C15 (see Figure 4). As evident from Figure 3B, the band at 1181 cm^{-1} (in H_2O) is the only fingerprint mode that experiences a noticeable downshift upon either C14 or C14,-15 labeling. Most of the C14−C15 stretching mode of the chromophore must therefore be comprised in the band located at 1182 cm^{-1}. In D_2O, the same applies to the two bands at 1247 and 1236 cm^{-1}. Closer examination of the decay of Meta II, under conditions where only negligible amounts of Meta III are being formed, indicates that splitting into this doublet is very likely caused by an interfering positive narrow Meta II band located at 1240 cm^{-1}, such that the position of the true Meta III band is likely to be found slightly above 1240 cm^{-1}.

The effect of H/D exchange at the protonated Schiff base can therefore be summarized as follows: there is a disappearance of the 1349 cm^{-1} band in D_2O and a very strong upshift of the frequency of the C14−C15 stretching mode by more than 50 cm^{-1}. This matches previously reported characteristics of the protonated 13-cis-15-syn chromophore in dark-adapted bacteriorhodopsin (BR_{548}). In this species,

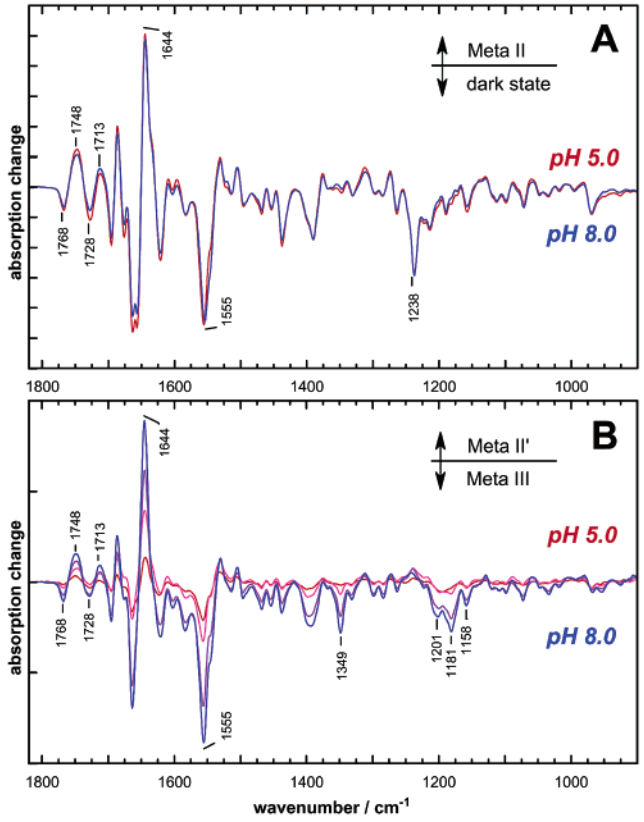

FIGURE 2: FTIR spectroscopic characterization of Meta III. FTIR difference spectra of the photoreactions from the dark state to Meta II at 30 °C at pH 5.0 and 8.0 (A) and of the subsequent photoreaction from Meta III to Meta II′ at pH 5.0, 6.0, 7.0, and 8.0 (red to blue) were obtained similarly as in Figure 1. Spectra in (A) and (B) were normalized by the intensity of the 1238 cm^{-1} band of the dark state in the initial dark state to Meta II difference spectra of each experiment. Please note the different ordinate scale in (A) and (B), which is 3-fold enlarged in (B); tick marks represent 1 mOD.

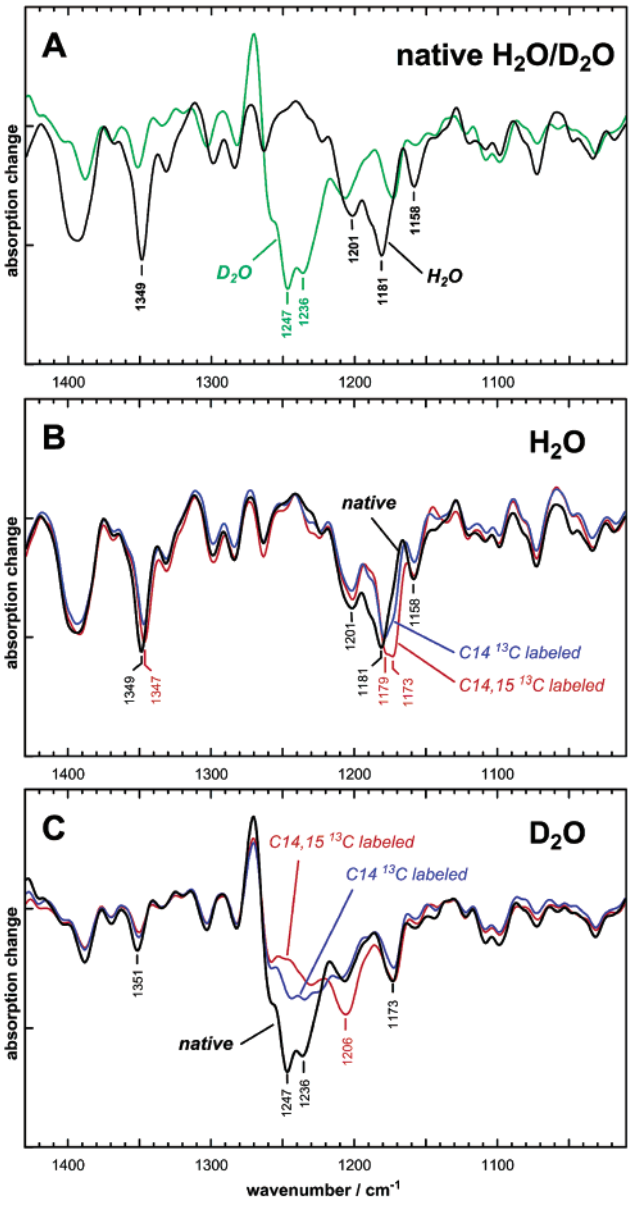

FIGURE 3: Characterization of Meta III fingerprint bands. Meta III to Meta II′ difference spectra are shown for native rhodopsin in H_2O and D_2O in the range of the fingerprint modes of the chromophore. In this representation, fingerprint bands associated with Meta III are negative. H/D exchange at the protonated Schiff base leads to a severe reduction of the 1349 cm^{-1} band of the NH bending mode and a dramatic upshift of the 1181 cm^{-1} fingerprint band of the C14−C15 stretch mode to a doublet at 1247 and 1236 cm^{-1} (A). The identity of the fingerprint bands was probed by their sensitivity to ^{13}C labeling of either C14 or both C14,15, as determined in H_2O (B) and D_2O (C). The labeling shows that the stretching mode of the C14−C15 single bond is mainly comprised in the 1181 cm^{-1} band in H_2O and in the 1247/1236 cm^{-1} doublet in D_2O. All spectra in this figure were normalized as in Figure 2; tick marks correspond to 0.5 mOD.

a very pronounced kinetic coupling between the C14−C15 stretching and the Schiff base NH bending vibrations can be observed, leading to a band located at 1345 cm^{-1} for the NH bending mode and to a reduced frequency of 1167 cm^{-1} for the C14−C15 vibration, as determined by resonance Raman spectroscopy (*38*, *39*). Upon H/D exchange at the Schiff base the 1345 cm^{-1} band of the NH bend shifts below 1000 cm^{-1} and becomes thus the lower frequency component of the pair. This reversion leads to a concomitant upshift of the frequency of the C14−C15 stretching mode by 41 cm^{-1}. Normal mode calculations on a six-atom protonated Schiff base fragment and on complete retinal-protonated Schiff bases indicated that such a strong H/D effect can be explained by vibrational coupling only if the Schiff base C═N is in a syn configuration, while in an anti configuration, only small (5−12 cm^{-1}) upshifts can be observed (*38*, *39*).

Vibrational Analysis from Quantum Chemical Calculations. With the development of density functional theory (DFT) highly accurate calculations of vibrational spectra have become accessible for organic dye molecules, as long as they are isolated in the gas phase (see, e.g., refs *40* and *41*). However, when placed into the binding pocket of a protein, the vibrational modes of a dye can become strongly modified by specific electrostatic interactions. Nonella et al. give an example for a corresponding vibrational mode calculation, which accounts for such effects and, therefore, had to be based on a given protein structure (*42*). Unfortunately, such a structure is missing for the Meta III state of rhodopsin. For the vibrational analysis of the Meta III chromophore we therefore had to use strongly simplified models, which replace a microscopic description of the protein environment by the vacuum or by a single counterion. Similar models have been previously used for the vibrational analysis of the retinal chromophore of bacteriorhodopsin (BR) (*43*). Due

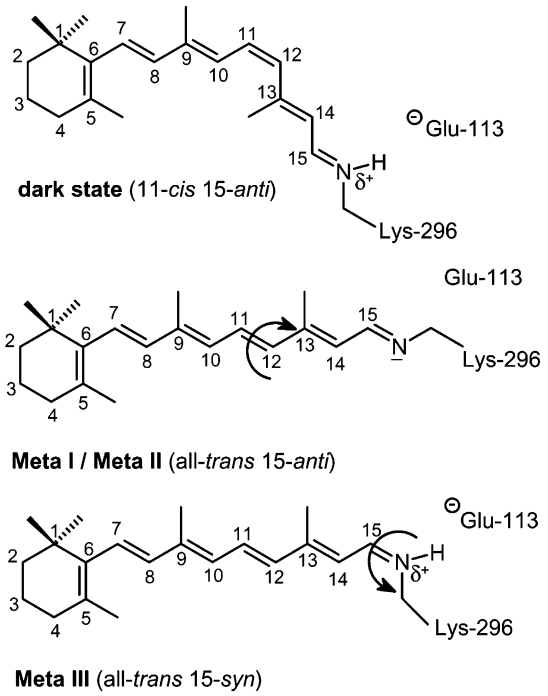

FIGURE 4: Structure of the retinal chromophore in the dark state and in the Meta states.

to these simplifications our computations can solely account for the dependence of vibrational bands on the isomeric state of the chromophore but cannot be expected to quantitatively match experimental spectra.

Our first aim was to determine the isomeric state of the C15═N bond. For this purpose we have examined the coupling of the NH in-plane bend to the C14−C15 single bond stretch in the all-trans isomer of the protonated model chromophore (without counterion), since previous normal mode calculations had suggested that this coupling should be indicative for 15-syn and 15-anti isomers (*38*, *39*). To take into account a putative thermal isomerization around the C13═C14 double bond, the same analysis was performed as well for the 13-cis isomer of this model chromophore.

Figure 5A displays the resulting frequencies, relative IR intensities, mode compositions, and frequency shifts upon Schiff base deuteration for the energetically lowest three C−C modes, which generate the so-called fingerprint band pattern. For these fingerprint modes a twofold pattern emerges: In the case of the two 15-anti isomers, the modes are nearly unaffected by the H/D exchange, whereas in the case of the two 15-syn isomers blue shifts of up to 27 cm^{-1} appear, particularly for the modes with a dominant C14−C15 stretch character. In Figure 5 these modes are marked by a star. These H/D shifting patterns of the C14−C15 modes in the 15-anti and 15-syn isomers, respectively, agree with the predictions and observations for the retinal chromophore in bacteriorhodopsin by Smith et al. (*38*, *39*, *44*). Although the calculated blue shifts of the C14−C15 modes in the 15-syn geometries of 27 and 18 cm^{-1} for all-trans and 13-cis, respectively, are somewhat smaller than the experimental values of more than 40 cm^{-1} observed in Meta III (see above) and BR_{548} (*39*), which is known to be 13-cis-15-syn, we can safely conclude that in Meta III the isomeric state of the C15═N bond of the chromophore is 15-syn.

Thus it remains to be decided whether our model calculations can also give a clue to the isomeric state of the

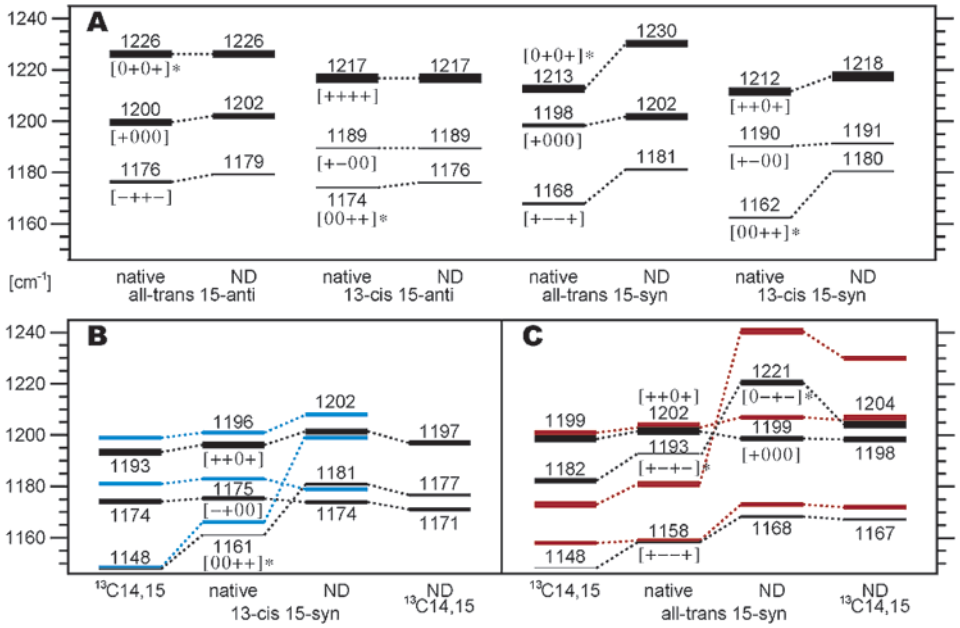

FIGURE 5: C−C mode frequencies calculated for models of the Meta III chromophore. The term schemes calculated for the fingerprint C−C modes are drawn in black. They are labeled by the isomeric states and isotope substitutions. The line thickness indicates the relative IR intensity of the respective mode. The phase relations of the C8−C9, C10−C11, C12−C13, and C14−C15 stretches are indicated at each normal mode by (+) for an in-phase coupling, (−) for a counter-phase coupling, and (0) for no coupling; e.g., [+000] is a pure C8−C9 stretching mode. The mode with the largest C14−C15 contribution is marked by a (*). Dotted lines connect modes of related phase combinations. (A) ND shifts for the four isomers. In the calculation no counterion was included. (B) Comparison of the 13-cis-15-syn counterion results with resonance Raman data for this isomer in BR_{548} [blue lines (*38*)]. (C) Comparison of the all-trans-15-syn counterion result with a mode assignment of the observed FTIR bands of the different isotopomers in Meta III (red lines; cf. Figure 3). Note that we have combined the two peaks at 1236 and 1247 cm^{-1} in the ND spectrum in Figure 3A into a single band at 1240 cm^{-1}, since the splitting of the band is most probably an artifact of difference spectroscopy as described in the text.

C13═C14 double bond in Meta III. Comparing the spectral positions of the C14−C15 stretches in Figure 5A, we find these modes to be the lowest in the two 13-cis isomers, whereas they are the highest in the all-trans isomers. The coupling patterns and spectral positions of the remaining two fingerprint modes are identical in the various 13-cis and all-trans isomers, respectively. Whether these spectral structures determined here for the cationic vacuum models can be considered to be indicative for the isomeric state of the C13═C14 double bond in the Meta III pRSB is unclear, because the protein electrostatics may strongly alter the force constants of the C−C bonds (*43*) and, thereby, change the spectral positions of the corresponding fingerprint modes. To estimate the influence of the protein electrostatics on the positions of these bands, we have placed a counterion close to the Schiff base, both for the all-trans-15-syn and the 13-cis-15-syn isomers. Clearly, we are aware that in rhodopsin possibly two negative charges (Glu-113 and Glu-181) are located in the vicinity of the pRSB. But since the exact locations of these residues relative to the pRSB in Meta III are unknown, we had to resort to the most simple one-counterion case.

Figure 5B shows the calculated vibrational frequencies for the 13-cis-15-syn isomer and for its various isotopomers. Furthermore, it compares these data with resonance Raman results obtained for this isomer in BR_{548} (*39*) to check the quality of our counterion calculations. The frequencies, the shifts upon isotopic labeling, as well as the coupling pattern of the experimental data are very well reproduced. An exception is the H/D shift of the C14−C15 mode at 1161 cm^{-1}, which is calculated at 20 cm^{-1} and, therefore, is underestimated by the same factor as in the cationic model. As compared to this model, the inclusion of the counterion leaves the C14−C15 frequency unaffected, whereas it shifts the remaining C−C stretches by about 15 cm^{-1} to the red (see Figure 5A,B). Note that the coupling patterns and spectral sequence of all fingerprint modes are preserved.

Turning to the effect of the counterion in the all-trans-15-syn isomer, we consider Figure 5C, which compares the calculated frequencies with band positions observed in Meta III (cf. Figure 3). By comparison with Figure 5A, we see that the counterion leads to a red shift of 5−11 cm^{-1} for all modes. The composition of the lowest mode does not change significantly, but the two upper modes become coupled upon the inclusion of the counterion. Particularly the mode at 1193 cm^{-1} gains a large C14−C15 contribution, which becomes larger than the one to the 1202 cm^{-1} mode. This mode composition is also witnessed by the large $^{13}C14,^{13}C15$ isotope effect of the mode at 1193 cm^{-1}. Note here that in the 13-cis isomer a C14−C15 character is exclusively found in the energetically lowest fingerprint mode (Figure 5B).

Upon deuteration of the Schiff base the two upper modes decouple in all-trans, and the 1193 cm^{-1} mode shifts by 28 cm^{-1} to the blue. As in the 13-cis-15-syn isomer (20 cm^{-1}), this blue shift is smaller than the experimental shift of more than 40 cm^{-1}. Nevertheless, the C14−C15 mode becomes the highest fingerprint mode upon this ND shift in all-trans as is witnessed by the sizable red shift upon additional $^{13}C14,^{13}C15$ substitution (last column in Figure 5C). This is quite in contrast to the 13-cis case, in which the energetically highest C−C mode of the ND isotopomer shows only a small $^{13}C14,^{13}C15$ isotope effect (last column of Figure 5B).

Table 1: Percentage of Retinal Oxime Isomers[a] Obtained by HPLC Analysis

	all-trans	13-cis
Meta II	99	1
Meta III	97	3
control expt: rhodopsin + 13-*cis*-retinal (50.9%) and all-*trans*-retinal (49.1%)[b]	50	50

[a] Syn and anti oximes were added. [b] Ratio of all-*trans*- and 13-*cis*-retinal incubated with rhodopsin is as indicated in parentheses. The extraction of the mixture gave also the 11-cis isomer from rhodopsin, which is not shown.

As discussed further above, for Meta III the $^{13}C14,^{13}C15$ isotope substitution has demonstrated that the C14−C15 stretch is not the energetically lowest, as expected for a 13-cis isomer (cf. Figure 5B), but a higher energy fingerprint band, as expected for all-trans (cf. Figure 5C). As shown by the red lines in the last two columns of Figure 5C, in Meta III the H/D exchange leads to a strong and very high frequency C14−C15 stretch, whose character is proven by the large $^{13}C14,^{13}C15$ isotope effect. A comparably large $^{13}C14,^{13}C15$ shift is seen for the topmost C−C mode of our deuterated model compound in these columns. As noted above, no such $^{13}C14,^{13}C15$ shift is predicted by our calculations for the topmost mode of the 13-cis isomer (Figure 5B). These findings lead us to conclude that the Meta III chromophore is an all-trans isomer. Together with the result on the isomeric state of the C═N bond derived further above, the vibrational analysis of the FTIR spectra has thus shown that the pRSB is all-trans-15-syn in Meta III.

Chromophore Extraction and Analysis. This assignment has been further confirmed experimentally by extraction and HPLC analysis of the retinal chromophore from Meta III, using Meta II as a control. The retinal was extracted as retinal oxime since this method was shown to prevent retinal isomerization during the extraction procedure (*45*). For the same reason, the extractions were carried out at 0 °C. As summarized in Table 1, Meta II yielded about 99% all-*trans*- and ca. 1% 13-*cis*-retinal. The latter probably originated from some residual isomerization of all-*trans*-retinal during the extraction procedure. The extractions of the retinal chromophore from Meta III were carried out under conditions where at least 40% of Meta III were present in the mixture. It was clearly observed that the mixture consisted of 97% all-*trans*-retinal. These results indicate that the retinal chromophore in Meta III adopts an all-trans configuration. However, the possibility that a potential 13-cis isomer isomerizes very fast and efficiently during its short incubation with the membrane mixture cannot be completely excluded by these experiments. To verify this possibility, we have therefore incubated rhodopsin (characterized by the 11-*cis*-retinal isomer) with 1 equiv of retinal consisting of a mixture of equal amounts of all-*trans*- and 13-*cis*-retinals. Subsequent extraction of the retinals revealed that there was no significant 13-cis to all-trans isomerization during the incubation and extraction process. The extracted isomeric mixture reflected the mixture that was initially incubated with rhodopsin. Therefore, it can be concluded that Meta III consists of an all-*trans*-retinyl chromophore.

Influence of the Lipid/Detergent Environment on the Meta III Yield. All previous experiments were conducted with

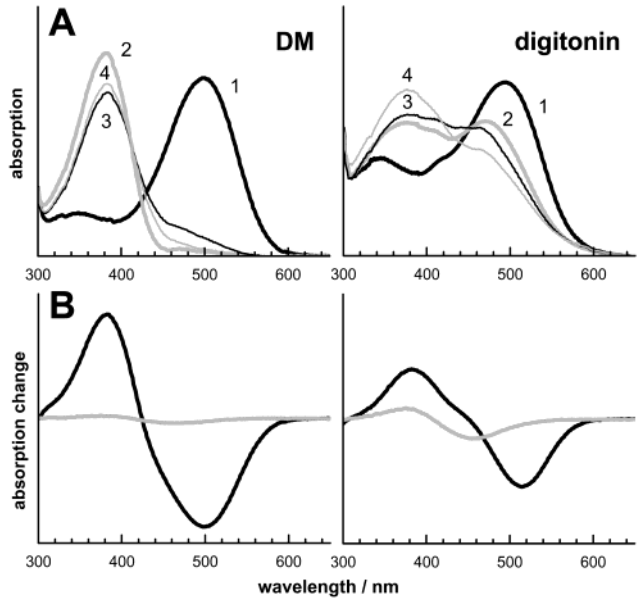

FIGURE 6: Influence of detergents on the Meta III yield. UV−vis spectroscopy was performed at 20 °C and pH 7.0 on rhodopsin solubilized in 0.1% dodecyl maltoside (DM) or 1% digitonin. (A) Illumination of the dark state (spectrum 1) leads to full formation of Meta II (in the case of DM) or to the establishment of a Meta I/Meta II equilibrium (in digitonin) (spectrum 2). These photoproducts decay fully within 40 min (spectrum 3). Subsequent illumination photolyzes Meta III, which again forms either Meta II (in the case of DM) or a Meta I/Meta II equilibrium (in digitonin) (spectrum 4). (B) Comparison of the difference spectra dark state to Meta II (black) and Meta III to Meta II′ (gray). The difference spectra were corrected as described in the text.

rhodopsin in its native lipid bilayer. Is the formation of Meta III altered if we replace this membranous environment by a detergent micelle? And to what extent is the pH-dependent formation of Meta III influenced by the Meta I/Meta II photoproduct equilibrium? To examine this, we compared formation of Meta III at same pH but in two detergents, dodecyl maltoside and digitonin, which affect the Meta I/Meta II equilibrium very differently. At the same pH and temperature, digitonin is known to be capable of stabilizing Meta I, while dodecyl maltoside strongly favors Meta II. Due to the lowered stability of the photoproducts in detergents toward denaturation (*46*), we investigated Meta III formation at 20 °C and pH 7.0 (Figure 6A) and corrected the spectra obtained from the second illumination for residual rhodopsin and isorhodopsin from the photoequilibrium of the first illumination as described in Materials and Methods. Under these conditions and in dodecyl maltoside, illumination of rhodopsin leads to formation of Meta II. During the decay of the photoproduct, only about 4% decay via Meta III, as deduced from a comparison of the absorption of the 380 nm peak in the Meta III to Meta II′ difference spectrum with that in the dark state to Meta II spectrum (Figure 6B). Parallel FTIR experiments reveal approximately 2.5% Meta III, as judged from the intensity of the negative band at 1349 cm^{-1} (not shown).

In contrast in digitonin, we observe after rhodopsin photolysis the establishment of a Meta I/Meta II equilibrium with approximately equal contributions of both species. After complete decay of this Meta I/Meta II pool, subsequent illumination of the decay product Meta III reproduces a mixture of species corresponding to Meta I/Meta II, similar to that obtained following the first illumination. Due to this correspondence, an identity of Meta II and Meta II′ and their Meta I precursors seems very likely. The more complicated bleaching behavior and the presence of residual rhodopsin and isorhodopsin after the first illumination (see Materials and Methods), however, hamper an accurate determination of the Meta III yield. An estimate can be made by comparison of the 380 nm peaks in both dark state to Meta II and Meta III to Meta II′ difference spectra (Figure 6B), similar to the case of dodecyl maltoside. This gives a Meta III yield of about 26% in digitonin.

Despite of the above-mentioned uncertainties, these data reveal a clear correlation between formation of Meta III and the presence of Meta I in the initial photoproduct equilibrium at a given temperature and pH. They support the notion that the increasing Meta III yield in disk membranes under more alkaline conditions (Figures 1C and 2B) is a consequence of the pH dependence of the Meta I/Meta II equilibrium.

Influence of the Schiff Base Protonation State on the Yield of Meta III. In an additional experiment we compared the decay of regular Meta II (Meta II_{380}) with that of Meta II with protonated Schiff base (Meta II_{PSB}). Protonation of the Schiff base in the latter Meta II species can be induced in the presence of suitable anions at low pH (*47*). We stabilized Meta II_{PSB} at pH 4.0 in the presence of 100 mM NaSCN at both 20 and 30 °C. Despite the reprotonation of the Schiff base, the yield of Meta III during the decay process was not enhanced compared to regular Meta II_{380}, as examined with FTIR spectroscopy (data not shown). The increased yield of Meta III in the presence of Meta I can therefore *not* be explained solely in terms of the protonated Schiff base in Meta I (in contrast to Meta II) and a thereby putatively lowered barrier for the thermal isomerization process.

Decay of Meta III and Stability toward Hydroxylamine. In agreement with previous studies (*15*, *16*), we observe a slow thermal decay of Meta III, which is evident in Figure 7A as a gradual decrease of the absorption peak at 470 nm with a time constant of 33 min. A similar decay of Meta III was observed with permethylated rhodopsin, where slow thermal reactions of peripheral Schiff bases of released retinal can be excluded. Release of free retinal is expected to lead to a concomitant substantial increase at 385 nm in the decay spectra as observed previously in a UV−vis study (*15*). The lack of a comparable prominent increase at 385 in our spectra is, however, understandable if one considers the oriented nature of our samples: in sandwich samples, the flat disk membranes form a film in which the membrane bilayers are aligned largely parallel to the window surface and thus perpendicular to the beam of light in the spectrometer. The orientation of the dipole moment of the chromophore in the dark state, Meta II, and Meta III is nearly parallel to the membrane plane (*16*) and yields, therefore, an absorption coefficient which is apparently increased compared to, e.g., unoriented suspensions. A vanishing absorption coefficient of released retinal, on the other hand, can be explained by a preferential orientation of retinal perpendicular to the membrane plane, i.e., parallel to the lipid acyl chains. Such an orientational change during retinal release has been reported previously (*12*) and is further supported by linear dichroism experiments (*16*).

We further tested the stability of Meta III toward hydroxylamine by the following experiment: We illuminated suspen-

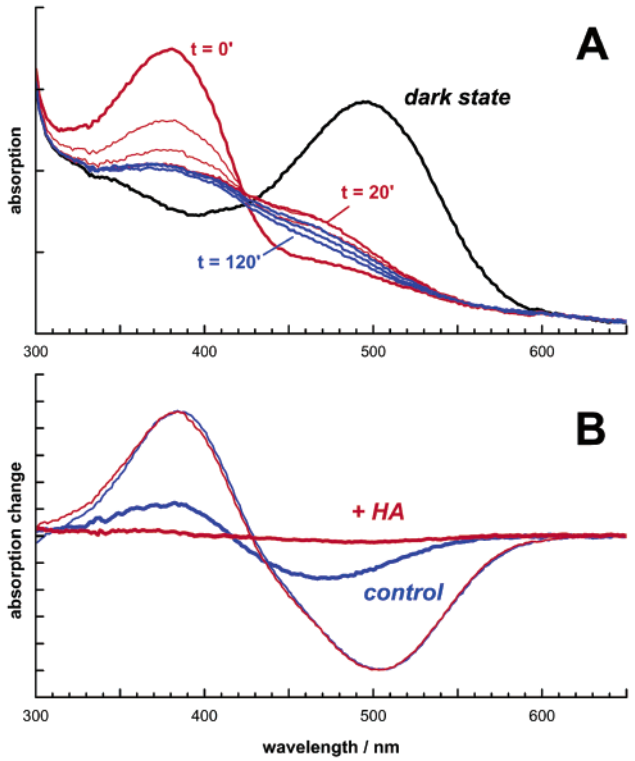

FIGURE 7: Decay of Meta III and stability toward hydroxylamine. (A) The stability of Meta III was tested in sandwich samples at 30 °C and pH 7.0. Illumination of the dark state of rhodopsin (black) leads to formation of largely Meta II (red, $t = 0$), which subsequently decays within 20 min and leads to the absorption increase of Meta III at 470 nm (red spectra, $t = 4$, 8, and 20 min). In the following, the 470 nm absorption decreases again slowly as shown in the blue spectra ($t = 40$, 60, and 120 min). (B) The stability of Meta III toward hydroxylamine was assayed in membrane suspensions at 30 °C and pH 7.0. Disk membranes were bleached to give largely Meta II (thin dark state to Meta II difference spectra). After full decay of the photoproducts within 20 min, 50 mM buffered hydroxylamine was added to one sample, while the control remained untreated. After another 5 min, both samples were illuminated again to give Meta III to Meta II′ difference spectra (thick spectra). In the hydroxylamine treated sample (+HA, red spectra), Meta III had been fully hydrolyzed within 5 min, such that its Meta III to Meta II′ difference spectrum is essentially zero, while the corresponding spectrum of the control sample (blue) shows the regular amount of Meta III that can be obtained under these conditions.

sions of disk membranes (Figure 7B, thin lines), followed by a decay of the photoproducts for 20 min to yield Meta III and released retinal. We then added 50 mM hydroxylamine and incubated the sample for another 5 min. The amount of pigment that was stable toward hydroxylamine was probed by a second illumination (Figure 7B, thick lines). In a control experiment (gray spectra), hydroxylamine was not added, and therefore, full Meta III content was obtained in the second difference spectrum. Obviously, Meta III had decayed rapidly upon hydroxylamine treatment with a time constant of less than 2 min, while the dark state of rhodopsin is found to be fully stable under our experimental conditions.

DISCUSSION

In this study we provide evidence that a thermal isomerization step of the retinal chromophore leads to the deactivation of rhodopsin's signaling state, Meta II, by triggering the transition to the inactive Meta III state. This evidence is based on an analysis of the chromophore structure in the Meta III state using FTIR difference spectroscopy on rhodopsins reconstituted with isotopically labeled retinals.

In the dark state, rhodopsin's 11-*cis*-retinal chromophore is bound to lysine 296 on helix 7 via a protonated Schiff base characterized by a 15-anti C═N double bond geometry (Figure 4) (*36*, *48*). This has been corroborated recently by solving the 3D structure of rhodopsin's dark state by X-ray diffraction (*49*, *50*).

Isomerization around C11═C12 during the photoreaction does not change the geometry of the C═N double bond, which remains 15-anti. This has been verified by analyzing the sensitivity of the C14−C15 stretch frequency for H/D exchange: Neither in Batho (*36*, *48*), nor in the likewise inactive Meta I state (*51*), nor in the active Meta II state (see Supporting Information) can a pronounced H/D shift of this frequency be observed.

In Meta III, on the other hand, we have observed upon H/D exchange a very pronounced upshift of the frequency of the C14−C15 stretching mode by more than 50 cm^{-1}. This upshift is caused by a very pronounced kinetic coupling between the C14−C15 stretching and the NH in-plane rocking mode. Previous results based on simple empirical force fields (*38*) as well as our own high-level DFT calculations show that such a strong H/D effect can be explained only when the Schiff base C═N adopts a syn (cis) configuration, as depicted in Figure 4. In addition, the DFT results collected in Figure 5B,C demonstrate that the ^{13}-C14,^{13}C15 isotope effects, which we observed in the FTIR spectra of Meta III for protonated and for deuterated chromophores, match the shifting patterns predicted for all-trans and fail to agree with those calculated for 13-cis. Here, the key point is that in 13-cis the C14−C15 stretch is the lowest frequency fingerprint mode, whereas this mode is shifted toward higher frequencies in all-trans. Thus our DFT vibrational analysis has revealed the Meta III chromophore to be an all-trans-15-syn isomer.

This is further underlined by chromophore extraction and HPLC analysis, which clearly exclude isomerization of any retinal double bond and confirm thus that the retinyl moiety in Meta III is characterized by an all-trans configuration. The retinal chromophore was extracted as its hydroxylamine derivative which was shown previously to faithfully reflect the retinal configuration in rhodopsin (*45*). However, isomerization from 13-cis to all-trans has a low barrier relative to the other retinal double bonds. Furthermore, it was shown previously that 13-*cis*-retinal isomerizes relatively fast in the presence of phosphatidylethanolamine (*52*). Therefore, we excluded the possibility of efficient and fast isomerization of the C13═C14 double bond during the extraction procedure in a control experiment where we added 13-c*is*- and all-*trans*-retinal to rhodopsin before extraction. The results confirmed that the denaturation and extraction procedure did not affect the C13═C14 double bond configuration. Therefore, the C═N is the only double bond that can experience isomerization in the Meta II to Meta III transformation.

We note that previous synthetic model studies indicated that in solution a large H/D shift of the C14−C15 stretch occurs in the 13-*cis*-retinal and not in the all-*trans* configuration (*53*). However, the DFT calculations carried out at the present studies indicate that in the 13-cis isomer the C14−C15 stretch is localized in the lowest frequency mode,

whereas in all-*trans*-retinal it is distributed among several modes. This may allow for the H/D effect to be more clearly observed in the 13-cis isomer. In addition, electrostatic interactions may strongly affect the vibrational coupling in the trans geometry, but not in the cis.

What is the driving force for the Schiff base isomerization and the transition to Meta III? Meta II can be found in a conformational equilibrium with its inactive precursor Meta I, which is generally favored by alkaline pH (*30*). At acidic pH, which favors Meta II in the Meta I/Meta II photoproduct equilibrium, the rate constant for formation of Meta III seems to be very small, such that Meta II decays mainly via hydrolysis of the Schiff base to give opsin and free retinal. With increasing pH, the decay to Meta III begins to compete with the hydrolysis pathway, such that at pH 8.0 (at 30 °C) about 30% of the initial photoproduct decay to Meta III, instead of being directly hydrolyzed. At 30 °C, the pK_a of the initial Meta I/Meta II equilibrium can be extrapolated to be around 8.5 (ref *54* and our own observations). It seems, therefore, conceivable that Meta III formation is enhanced under conditions where the initial photoproduct equilibrium between Meta I and Meta II is not completely on the Meta II side, such that still some Meta I is present. This proposition was tested by comparing the yield of Meta III at identical pH but in two different detergents with different capabilities to stabilize Meta I in the initial photoproduct equilibrium. In dodecyl maltoside, which strongly favors Meta II over Meta I, only a tiny amount of Meta III could be detected after the decay process. In digitonin, on the other hand, the initial photoproduct consisted of an equilibrium mixture of both Meta I and Meta II under the chosen pH and temperature conditions of the assay. During the decay of this Meta I/Meta II pool, substantial formation of Meta III could be observed. This raises the possibility that the inactive Meta I conformation catalyzes formation of Meta III by decreasing the activation energy barrier of the necessary thermal isomerization step and/or by stabilizing considerably the C=N syn configuration. The possibility that the protein affects Meta III formation solely by increasing the pK_a of the protonated Schiff base and by inducing thereby Schiff base protonation can be excluded, as neither regular Meta II with deprotonated Schiff base (Meta II_{380}) nor Meta II with protonated Schiff base (Meta II_{PSB}) yielded substantial amounts of Meta III.

Other experiments further support a Meta II-independent formation of Meta III: In dry films of disk membranes, the cascade of photointermediates does not proceed to Meta II but allows only formation of the inactive states Lumi or Meta I (*55*). At room temperature, this inactive photoproduct decays directly to Meta III ,as evident from IR decay spectra (R. Vogel, F. Siebert, G. Fan, and M. Sheves, unpublished results). A similar formation of Meta III is observed for rhodopsin reconstituted into distearoylphosphocholine bilayers, where the transition to Meta II is blocked likewise (manuscript in preparation).

The thermal isomerization of the chromophore that leads to formation of Meta III seems therefore to be favored in the inactive protein conformation of Meta I. We can presume that the all-trans-15-anti chromophore, which constitutes a strong agonist, is not very much compatible with the binding pocket of an inactive receptor species such as Meta I. This situation can be relieved by specific reactions of either protein or chromophore: the protein may respond to the chromophore and adopt the both entropically and enthalpically higher conformation of the active Meta II state, or the chromophore can comply to its protein environment by the thermal isomerization around the C=N bond to adopt the all-trans-15-syn geometry of Meta III, which seems to be more stable in the binding pocket of an inactive receptor species. The protein can therefore be viewed as a catalyst, which controls the activation energy of the thermal isomerization step and which affects the relative stability of the syn and anti C=N configuration through specific steric chromophore−protein and possibly as well by defined hydrogen-bonding networks formed in the Schiff base vicinity in both isomers.

Meta III itself was found to be intrinsically unstable and to decay slowly. Previous studies reported that the transition from the Meta I/Meta II pool to Meta III pool is reversible (*14*, *16*). Obviously, Meta III could then decay via back-reaction to the Meta I/Meta II pool and subsequent hydrolysis of Meta II. However, in light of the pronounced sensitivity of Meta III toward hydroxylamine, a direct hydrolysis of Meta III to opsin and free all-*trans*-retinal seems possible as well in the decay process, despite that sensitivity toward hydroxylamine does not necessarily imply a fast hydrolysis reaction.

We thus arrive at the following scheme for the decay of the Meta I/Meta II photoproduct equilibrium:

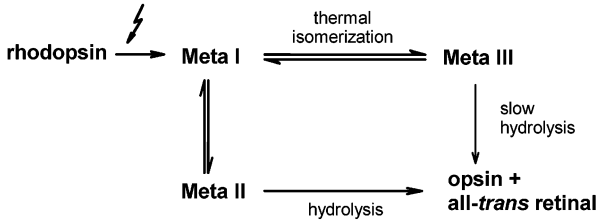

Photolysis of rhodopsin produces Meta I, which establishes a rapid (millisecond) equilibrium with the active receptor species Meta II. Decay of this Meta I/Meta II pool proceeds by two pathways: dissociation of the receptor into retinal and opsin after hydrolysis of the Schiff base link, which proceeds mainly via Meta II, or transition to Meta III following chromophore C=N bond thermal isomerization, which proceeds mainly via Meta I. Eventually, Meta III decays either via hydrolysis of the retinal Schiff base in the Meta I/Meta II pool or possibly as well via direct hydrolysis of the protonated Schiff base of Meta III (indicated as a possible pathway by the dotted arrow in the above scheme), the decay product being opsin and free all-*trans*-retinal in either case.

Thermal isomerization steps are commonly observed during the photocycles of the archaeal rhodopsins, as bacteriorhodopsin, halorhodopsin, or sensory rhodopsin, as well as in related proteins found recently also in eukaryotic organisms. These proteins serve as ion pumps or as sensory pigments that couple to specific bacterial transducer molecules. Despite being as well retinal-binding proteins and sharing a similar topology including seven membrane-spanning helices, they are distinctly different from the visual pigments, which are found exclusively in higher organisms, in respect to both their molecular organization and functional context.

Already in the classical 1963 paper of Wald and coworkers (*30*), the possibility is raised that the transition to Meta III is triggered by a thermal isomerization of the retinal chromophore within the native binding pocket. However, until recently, there had been no further evidence for thermal isomerization steps of the chromophore to be involved in the deactivation of visual pigments. Only the recently examined peculiar behavior of an artificial pigment, $Rho_{6.10}$, demonstrated that thermal isomerization may occur as well in visual pigments. $Rho_{6.10}$ contains a chromophore in which the C11═C12 double bond is locked in a cis position. Despite this "lock", the pigment can be activated by light (*22*, *56*), which by itself is not too astonishing after taking into account results from previous studies on the properties of opsin and of the chromophore alone (*12*, *57*). The most astonishing feature of this pigment is its capability to return thermally from the activated state back to the initial state, in which it was prior to photoexcitation (*2*, *58*). Most likely, this is achieved by a thermal isomerization of its chromophore about the C13═C14 double bond, thereby converting it from an activating, agonistic geometry to that of an inactivating inverse agonist. The thermal transition from Meta II to Meta III and the photoconvertibility of Meta III back to Meta II (i.e., the thermal and light-induced isomerizations of the C═N double bond, respectively) of native rhodopsin as well establishes some kind of photocycle. In contrast to that of the locked rhodopsin, however, this photocycle does not lead to full recovery of the initial state, as there is always the competing photoproduct decay via Schiff base hydrolysis, which is absent in the locked pigment. Furthermore, even the Meta III "ground state" itself is not stable but decays slowly.

ACKNOWLEDGMENT

We thank B. Mayer, W. Sevenich, W. D. Schielin, P. Merkt, and K. Zander for technical assistance, S. Lüdeke for critically reading the manuscript, and the reviewers for their critical suggestions.

SUPPORTING INFORMATION AVAILABLE

Analysis of fingerprint bands of Meta II. This material is available free of charge via the Internet at http://pubs.acs.org.

REFERENCES

1. Menon, S. T., Han, M., and Sakmar, T. P. (2001) Rhodopsin: structural basis of molecular physiology, *Physiol. Rev. 81*, 1659−1688.
2. Vogel, R., and Siebert, F. (2003) New insights from FTIR spectroscopy into molecular properties and activation mechanisms of the visual pigment rhodopsin, *Biospectroscopy 72*, 133−148.
3. Okada, T., Ernst, O. P., Palczewski, K., and Hofmann, K. P. (2001) Activation of rhodopsin: new insights from structural and biochemical studies, *Trends Biochem. Sci. 26*, 318−324.
4. Shichida, Y., and Imai, H. (1998) Visual pigment: G-protein-coupled receptor for light signals, *Cell. Mol. Life Sci. 54*, 1299−1315.
5. Schoenlein, R. W., Peteanu, L. A., Mathies, R. A., and Shank, C. V. (1991) The first step in vision: femtosecond isomerization of rhodopsin, *Science 254*, 412−415.
6. Helmreich, E. J. M., and Hofmann, K. P. (1996) Structure and function of proteins in G protein-coupled signal transfer, *Biochim. Biophys. Acta 1286*, 285−322.
7. Fain, G. L., Matthews, H. R., Cornwall, M. C., and Koutalos, Y. (2001) Adaptation in vertebrate photoreceptors, *Physiol. Rev. 81*, 117−151.
8. Papermaster, D. S. (1982) Preparation of retinal rod outer segments, *Methods Enzymol. 81*, 48−52.
9. Melia, T. J., Cowan, C. W., Angleson, J. K., and Wensel, T. G. (1997) A comparison of the efficiency of G protein activation by ligand-free and light-activated forms of rhodopsin, *Biophys. J. 73*, 3182−3191.
10. Rothschild, K. J., Gillespie, J., and DeGrip, W. J. (1987) Evidence for rhodopsin refolding during the decay of Meta II, *Biophys. J. 51*, 345−350.
11. Klinger, A. L., and Braiman, M. S. (1992) Structural comparison of metarhodopsin II, metarhodopsin III, and opsin based on kinetic analysis of Fourier transform infrared difference spectra, *Biophys. J. 63*, 1244−1255.
12. Vogel, R., and Siebert, F. (2001) Conformations of the active and inactive states of opsin, *J. Biol. Chem. 276*, 38487−38493.
13. Ostroy, S. E., Erhardt, F., and Abrahamson, E. W. (1966) Protein configuration changes in the photolysis of rhodopsin. II. The sequence of intermediates in thermal decay of cattle metarhodopsin in vitro, *Biochim. Biophys. Acta 112*, 265−277.
14. Kibelbek, J., Mitchell, D. C., Beach, J. M., and Litman, B. J. (1991) Functional equivalence of metarhodopsin II and the G_t-activating form of photolyzed bovine rhodopsin, *Biochemistry 30*, 6761−6768.
15. Lewis, J. W., van Kuijk, F. J., Carruthers, J. A., and Kliger, D. S. (1997) Metarhodopsin III formation and decay kinetics: comparison of bovine and human rhodopsin, *Vision Res. 37*, 1−8.
16. Chabre, M., and Breton, J. (1979) The orientation of the chromophore of vertebrate rhodopsin in the "Meta" intermediate states and the reversibility of the Meta II-Meta III transition, *Vision Res. 19*, 1005−1018.
17. van Breugel, P. J., Bovee-Geurts, P. H., Bonting, S. L., and Daemen, F. J. (1979) Biochemical aspects of the visual process. XL. Spectral and chemical analysis of metarhodopsin III in photoreceptor membrane suspensions, *Biochim. Biophys. Acta 557*, 188−198.
18. Reuter, T. (1976) Photoregeneration of rhodopsin and isorhodopsin from metarhodopsin III in the frog retina, *Vision Res. 16*, 909−917.
19. Heck, M., Schädel, S. A., Maretzki, D., Bartl, F. J., Ritter, E., Palczewski, K., and Hofmann, K. P. (2003) Signaling states of rhodopsin. Formation of the storage form, metarhodopsin III, from active metarhodopsin II, *J. Biol. Chem. 278*, 3162−3169.
20. Bartl, F. J., Ritter, E., and Hofmann, K. P. (2001) Signaling states of rhodopsin: absorption of light in active Metarhodopsin II generates an all-*trans*-retinal bound inactive state, *J. Biol. Chem. 276*, 30161−30166.
21. Vogel, R., Fan, G. B., Sheves, M., and Siebert, F. (2000) The molecular origin of the inhibition of transducin activation in rhodopsin lacking the 9-methyl group of the retinal chromophore: A UV−vis and FTIR spectroscopic study, *Biochemistry 39*, 8895−8908.
22. Fan, G. B., Siebert, F., Sheves, M., and Vogel, R. (2002) Rhodopsin with 11-*cis*-locked chromophore is capable of forming an active state photoproduct, *J. Biol. Chem. 277*, 40229−40234.
23. Delange, F., Bovee-Geurts, P. H., Vanoostrum, J., Portier, M. D., Verdegem, P. J., Lugtenburg, J., and DeGrip, W. J. (1998) An additional methyl group at the 10-position of retinal dramatically slows down the kinetics of the rhodopsin photocascade, *Biochemistry 37*, 1411−1420.
24. Longstaff, C., and Rando, R. R. (1985) Methylation of the active-site lysine of rhodopsin, *Biochemistry 24*, 8137−8145.
25. DeGrip, W. J. (1982) Purification of bovine rhodopsin over cancanavalin A-Sepharose, *Methods Enzymol. 81*, 197−207.
26. Becke, A. D. (1993) Density-Functional thermochemistry. III. The role of exact exchange, *J. Chem. Phys. 98*, 5648−5652.
27. Lee, C., Yang, W., and Parr, R. C. (1988) Development of the Colle-Salvetti correlation energy formula into a functional of the electron density, *Phys. Rev. B 37*, 785−789.
28. Frisch, M. J. (1998) *Gaussian 98*, Gaussian, Inc., Pittsburgh, PA.
29. Foresman, J. B., and Frisch, Æ. (1996) *Exploring chemistry with electronic structure methods*, Gaussian, Inc., Pittsburgh, PA.
30. Matthews, R. G., Hubbard, R., Brown, P. K., and Wald, G. (1963) Tautomeric forms of Metarhodopsin, *J. Gen. Physiol. 47*, 215−240.
31. Siebert, F. (1995) Application of FTIR spectroscopy to the investigation of dark structures and photoreactions of visual pigments, *Isr. J. Chem. 35*, 309−323.

32. Sakmar, T. P., Franke, R. R., and Khorana, H. G. (1989) Glutamic acid-113 serves as the retinylidene Schiff base counterion in bovine rhodopsin, *Proc. Natl. Acad. Sci. U.S.A. 86*, 8309−8313.
33. Jäger, F., Fahmy, K., Sakmar, T. P., and Siebert, F. (1994) Identification of glutamic acid 113 as the Schiff base proton acceptor in the Metarhodopsin II photointermediate of rhodopsin, *Biochemistry 33*, 10878−10882.
34. Rath, P., DeCaluwe, L. L., Bovee-Geurts, P. H., DeGrip, W. J., and Rothschild, K. J. (1993) Fourier transform infrared difference spectroscopy of rhodopsin mutants: light activation of rhodopsin causes hydrogen-bonding change in residue aspartic acid-83 during Meta II formation, *Biochemistry 32*, 10277−10282.
35. Fahmy, K., Jäger, F., Beck, M., Zvyaga, T. A., Sakmar, T. P., and Siebert, F. (1993) Protonation states of membrane-embedded carboxylic acid groups in rhodopsin and Metarhodopsin II: a Fourier transform infrared spectroscopy study of site-directed mutants, *Proc. Natl. Acad. Sci. U.S.A. 90*, 10206−10210.
36. Palings, I., Pardoen, J. A., van den Berg, E. M., Winkel, C., Lugtenburg, J., and Mathies, R. A. (1987) Assignment of fingerprint vibrations in the resonance Raman spectra of rhodopsin, isorhodopsin, and bathorhodopsin: implications for chromophore structure and environment, *Biochemistry 26*, 2544−2556.
37. Siebert, F., and Mäntele, W. (1980) Investigations of the rhodopsin/Meta I and rhodopsin/Meta II transitions of bovine rod outer segments by means of kinetic infrared spectroscopy, *Biophys. Struct. Mech. 6*, 147−164.
38. Smith, S. O., Myers, A. B., Pardoen, J. A., Winkel, C., Mulder, P. P. J., Lugtenburg, J., and Mathies, R. (1984) Determination of retinal Schiff base configuration in bacteriorhodopsin, *Proc. Natl. Acad. Sci. U.S.A. 81*, 2055−2059.
39. Smith, S. O., Pardoen, J. A., Lugtenburg, J., and Mathies, R. A. (1987) Vibrational analysis of the 13-*cis*-retinal chromophore in dark-adapted bacteriorhodopsin, *J. Phys. Chem. 91*, 804−819.
40. Nonella, M., and Tavan, P. (1995) An unscaled quantum mechanical force field for p-benzoquinone, *Chem. Phys. 199*, 19−32.
41. Zhou, X., Mole, S. J., and Liu, R. (1996) Density functional theory of vibrational spectra. 4. Comparison of experimental and calculated frequencies of all-*trans*-1,3,5,7-octatetraene—The end of normal coordinate analysis? *Vib. Spectrosc. 12*, 73−79.
42. Nonella, M., Mathias, G., Eichinger, M., and Tavan, P. (2003) Structures of vibrational frequencies of the quinones in *Rb. sphaeroides* derived by a combined density functional/molecular mechanics approach, *J. Phys. Chem. B 107*, 316−322.
43. Grossjean, M. F., Tavan, P., and Schulten, K. (1990) Quantum chemical vibrational analysis of the chromophore of bacteriorhodopsin, *J. Phys. Chem. 94*, 8059−8069.
44. Smith, S. O., Braiman, M. S., Myers, A. B., Pardoen, J. A., Courtin, J. M. L., Winkel, C., Lugtenburg, J., and Mathies, R. A. (1987) Vibrational analysis of the all-trans-retinal chromophore in light-adapted bacteriorhodopsin, *J. Am. Chem. Soc. 109*, 3108−3125.
45. Groenendijk, G. W., De Grip, W. J., and Daemen, F. J. (1980) Quantitative determination of retinals with complete retention of their geometric configuration, *Biochim. Biophys. Acta 617*, 430−438.
46. Vogel, R., and Siebert, F. (2002) Conformation and stability of α-helical membrane proteins. 2. Influence of pH and salts on stability and unfolding of rhodopsin, *Biochemistry 41*, 3536−3545.
47. Vogel, R., Fan, G. B., Siebert, F., and Sheves, M. (2001) Anions stabilize a Metarhodopsin II-like photoproduct with a protonated Schiff base, *Biochemistry 40*, 13342−13352.
48. Bagley, K. A., Balogh-Nair, V., Croteau, A. A., Dollinger, G., Ebrey, T. G., Eisenstein, L., Hong, M. K., Nakanishi, K., and Vittitow, J. (1985) Fourier transform infrared difference spectroscopy of rhodopsin and its photoproducts at low temperature, *Biochemistry 24*, 6055−6071.
49. Palczewski, K., Kumasaka, T., Hori, T., Behnke, C. A., Motoshima, H., Fox, B. A., Le Trong, I., Teller, D. C., Okada, T., Stenkamp, R. E., Yamamoto, M., and Miyano, M. (2000) Crystal structure of rhodopsin: A G protein-coupled receptor, *Science 289*, 739−745.
50. Okada, T., Fujiyoshi, Y., Silow, M., Navarro, J., Landau, E. M., and Shichida, Y. (2002) Functional role of internal water molecules in rhodopsin revealed by x-ray crystallography, *Proc. Natl. Acad. Sci. U.S.A. 99*, 5982−5987.
51. Pan, D., and Mathies, R. A. (2001) Chromophore structure in Lumirhodopsin and Metarhodopsin I by time-resolved resonance Raman microchip spectroscopy, *Biochemistry 40*, 7929−7936.
52. Groenendijk, G. W., Jacobs, C. W., Bonting, S. L., and Daemen, F. J. (1980) Dark isomerization of retinals in the presence of phosphatidylethanolamine, *Eur. J. Biochem. 106*, 119−128.
53. Livnah, N., and Sheves, M. (1993) The Schiff base bond configuration in bacteriorhodopsin and in model compounds, *Biochemistry 32*, 7223−7228.
54. Parkes, J. H., and Liebman, P. A. (1984) Temperature and pH dependence of the Metarhodopsin I−Metarhodopsin II kinetics and equilibria in bovine rod disk membrane suspensions, *Biochemistry 23*, 5054−5061.
55. Nishimura, S., Sasaki, J., Kandori, H., Lugtenburg, J., and Maeda, A. (1995) Structural changes in the lumirhodopsin-to-metarhodopsin I conversion of air-dried bovine rhodopsin, *Biochemistry 34*, 16758−16763.
56. Kuksa, V., Bartl, F., Maeda, T., Jang, G. F., Ritter, E., Heck, M., Van Hooser, J. P., Liang, Y., Filipek, S., Gelb, M. H., Hofmann, K. P., and Palczewski, K. (2002) Biochemical and physiological properties of rhodopsin regenerated with 11-*cis*-6-ring and 7-ring-retinals, *J. Biol. Chem. 277*, 42315−42324.
57. Jang, G. F., Kuksa, V., Filipek, S., Bartl, F., Ritter, E., Gelb, M. H., Hofmann, K. P., and Palczewski, K. (2001) Mechanism of rhodopsin activation as examined with ring-constrained retinal analogues and the crystal structure of the ground-state protein, *J. Biol. Chem. 276*, 26148−26153.
58. Vogel, R., Fan, G. B., Lüdeke, S., Siebert, F., and Sheves, M. (2002) A nonbleachable rhodopsin analogue with a slow photocycle, *J. Biol. Chem. 277*, 40222−40228.

BI034684+